Discovery and nano-sized preparations of (*S*, *R*)-tylophorine malate as novel anti-SARS-CoV-2 agents

Ziwen Wang[a,d,§], Fei Ye[b,§], Yue Feng[c], Wen Xiao[c], Hongjian Song[a,*], Li Zhao[b], Roujian Lu[b], Baoying Huang[b], Yuxiu Liu[a], Wenling Wang[b], Yongqiang Li[a], Yi Ding[a,e], Yanlong Zheng[a], Xiangrong Song[c,*], Wenjie Tan[b,*], Qingmin Wang[a,*]

[a]State Key Laboratory of Elemento-Organic Chemistry, Research Institute of Elemento-Organic Chemistry, College of Chemistry, Frontiers Science Center for New Organic Matter, Nankai University, Tianjin 300071, China.

[b]NHC Key Laboratory of Biosafety, National Institute for Viral Disease Control & Prevention, Chinese Center for Disease Control and Prevention, China CDC, Beijing 102206, China.

[c]Department of Critical Care Medicine, Frontiers Science Center for Disease-related Molecular Network, State Key Laboratory of Biotherapy and Cancer Center, West China Hospital, Sichuan University, Chengdu 610041, China.

[d]Tianjin Key Laboratory of Structure and Performance for Functional Molecules, College of Chemistry, Tianjin Normal University, Tianjin Normal University, Tianjin 300387, China.

[e]Shijiazhuang Lvfeng Chemical Co., Ltd., Shijiazhuang 052560, China.
[§]Ziwen Wang and Fei Ye contributed equally to this work.

Correspondence to: wangqm@nankai.edu.cn (Q. W.); songhongjian@nankai.edu.cn (H. S.); tanwj@ivdc.chinacdc.cn (W. T.); songxr@scu.edu.cn (X. S.)

Contents

Materials and Methods

Chemicals

Reagents were purchased from commercial sources and were used as received. All anhydrous solvents were dried and purified by standard techniques prior to use. The *S*-tylophorine was synthesized by means of our reported method (*1*). mPEG-PLGA (MW = 15 kDa; LA/GA = 75:25; PEG MW = 2 kDa) was purchased from Jinan Daigang Biomaterial Co., Ltd. (Jinan, China). Poly (vinyl alcohol) (PVA, MW=30–70 kDa, HD, 80%). 1,2-dioleoyl-3-trimethylammonium-propane (DOTAP) was purchased from Avanti Polar Lipids Inc. (Alabaster, USA). Cholesterol (CHOL) and the lipophilic fluorescent dye DiD were obtained from Shanghai boao biotechnology Co. Ltd. (Shanghai, China). Other lipids were synthesized by our laboratory.

Instruments

The melting point of NK007(*S*, *R*) was determined on an X-4 binocular microscope (Beijing Tech Instruments Company). ^{1}H NMR spectrum was obtained with a Bruker AV 400 spectrometer with DMSO-d_6 as the solvent.

Preparation of NK007(*S*, *R*)

A solution of *S*-tylophorine (0.39 g, 1 mmol) in CH_2Cl_2 (50 mL) was added dropwise to a solution of D-malic acid (0.13 g, 1 mmol) in CH_2Cl_2 (50 mL) and CH_3OH (50 mL). The reaction mixture was stirred at room temperature for 8 h and then filtered to obtain NK007(*S*,*R*) (0.51 g, 97%) as a yellow solid (mp 245–247 °C). ^{1}H NMR (400 MHz, DMSO-d_6) 8.10 (s, 2H), 7.41 (s, 1H), 7.26 (s, 1H), 4.85 (d, *J* =14.8 Hz,1H), 4.20–4.16 (m, 1H), 4.10 (s, 6H), 4.00 (s, 6H), 3.59–3.55 (m, 2H), 3.03–2.60 (m, 5H), 2.48–2.43 (m, 1H), 2.39–2.33 (m, 1H), 2.06–1.99 (m, 2H), 1.86–1.78 (m, 1H).

Preparation and characterization of NP-NK007

The self-assembled PEG-PLGA nanoparticle loaded with NK007(*S*, *R*) (NP-NK007) was prepared according to a double-emulsion (W1/O/W2) solvent evaporation method (*2*). Firstly, accurately weighed amounts of NK007(*S*,*R*) and mPEG-PLGA were dissolved in dichloromethane. Subsequently, the inner aqueous phase (purified water) was added to the organic phase and emulsified using a probe sonicator in an ice bath to obtain the primary (W1/O) emulsion. The W1/O emulsion was then added to the 4 mL external water phase solution and further sonicated to obtain the final $W_1/O/W_2$ double emulsion. Dichloromethane (DCM) was removed by rotary evaporation at 37 °C to obtain the colloidal solution NP-NK007.

Preparation of LP-NK007

The liposome loaded with NK007(*S*, *R*) (LP-NK007) was prepared by reverse-phase evaporation method. Briefly, the mixture of lipids in the organic phase and NK007(*S*, *R*) in the aqueous phase were sonicated for 6 min. Then, the organ solvent was fully removed by a rotary evaporator for 2 h at 37 °C. Purified water was added to hydrate for 1 h at 60 °C. Lipid suspension was subsequently sonicated for 3 min. LP-NK007 was finally obtained after filtering through 0.22 μm filter, and stored at 4 °C.

Particle Size and Zeta Potential

The mean particle size, size distribution and zeta potential were measured by Zetasizer (Zetasizer NanoZS 90) at 25 °C. The tested samples were diluted 10 times with purified water for measurements. Experiments were conducted in triplicate.

Entrapment Efficiency and Drug Loading

Briefly, the supernatant obtained from the ultrafiltration centrifuging of the colloidal suspension (NP-NK007 or LP-NK007) was stored to determine the encapsulation efficiency (EE) and drug

loading capacity (DL) as previously described (*2*). The NK007(*S*, *R*) in supernatant was measured by ultraviolet spectrophotometer (UV) analysis. The EE (%) and DL (%) were calculated according to the following equations 1 and 2: $\mathrm{EE}(\%) = \frac{\text{Amount of NK007}(S,R)\text{ in the preparation}}{Total\ NK007(S,R)\ amount} \times 100\%$ (1)

$\mathrm{DL}(\%) = \frac{\text{Amount of NK007}(S,R)\text{ in the preparation}}{Total\ weight\ of\ the\ preparation} \times 100\%$ (2)

In vitro Release Studies

The *in vitro* release profile of NP-NK007 was investigated in 0.5% tween-80 PBS buffer at pH 7.4 by dynamic dialysis method (*3*). In a word, free NK007(*S*, *R*) solution and NP-NK007 in dialysis bags (MWCO 3700) were first dispersed in the release media at 37 ^{o}C and then were shaken with a speed of 100 rpm. Release medium (1 mL) was taken out and replaced with equal volume fresh release medium at predetermined time intervals (1, 2, 3, 4, 6, 8, 12, 24, 48 h). The content of NK007(*S*, *R*) in the media was measured by UV spectrophotometry after centrifugation for 10 min at 13,000 rpm.

Biodistribution Studies of NP-NK007 and LP-NK007

C57BL/6 mice were used to investigate the organ biodistribution of the two nano-sized preparations. 200 μL of DiD solution, NP-DiD or LP-DiD colloidal suspension were injected into healthy mice via the tail vein, respectively. As for the control group, same volume physiological saline was administered to the mice. After 2 h, the mice were promptly sacrificed and the organs (liver, heart, spleen, lung and kidney) were harvested and imaged via a Quick View 3000 Bio-Real *in vivo* imaging system (Bio-Real, Austria).

Biological Assay

Animals

C57BL/6 mice (aged 6–8 weeks, male and weighed 22–25 g, SPF grade) were purchased from Dashuo Biotechnology Company, Ltd. (Chengdu, China). All the experiments on animals were

approved and supervised by the West China School of Pharmacy Animal Care and Use Committee (Sichuan University). All animals were kept in the environment of 12:12 hours light–dark cycle at the temperature 22 ± 1 °C and the relative humidity remained at 55 ± 10%.

Cell Culture and Virus Propagation

Vero cells were treated with drugs at different concentrations for 48 h in 5% CO_2 at 37 °C. Cell viability was tested by CellTiter96 One Solution Reagent (Promega, USA) assay. Briefly, 20 μL of One Solution Reagen was added to the medium and incubated with cells for 1-4 h. Absorbance value was measured at 490 nm wavelength using a microplate reader (Thermo Fisher Scientific, Waltham, USA). The 50% cytotoxic concentration (CC_{50}) was calculated by the GraphPad Prism 7.0 software.

Antiviral Activity Assay

We evaluated the activity of NK007(*S*, *R*) against SARS-CoV-2 (C-Tan-nCoV Wuhan strain 01) virus *in vitro*. Cells were seeded into 96-well plates at a density of 2×10^4 cells/well and then grown for 24 hours. The Vero cells were infected at a multiplicity of infection (MOI) of 0.01 (200 PFU/well) for 1 h at 37 ℃. Virus input was washed with DMEM and then the cells were treated with medium contained NK007(*S*, *R*) at various concentrations (5 μM, 0.5 μM, 0.05 μM, 0.005 μM, 0.0005 μM, 0.00005 μM) or remdesivir at concentrations (100 μM, 20 μM, 4 μM, 0.8 μM, 0.16 μM, 0.032 μM) for 48 h. The supernatant was collected and the RNA was extracted and analyzed by relative quantification by RT-PCR as previous study (*4*).

RNA Extraction and RT-qPCR

Viral RNA was extracted from 100 μL supernatant of infected cells using the automated nucleic acid extraction system (TIANLONG, China), following the manufacturer's recommendations. SARS-COV-2 virus detection was performed using the One Step PrimeScript RT-PCR kit

(TaKaRa, Japan) on the LightCycler 480 Real-Time PCR system (Roche, Rotkreuz, Switzerland). ORF 1ab was amplified from cDNA and cloned into MS2-nCoV-ORF1ab and used as the plasmid standard after its identify was confirmed by sequencing. A standard curve was generated by determination of copy numbers from serially dilutions (10^3-10^9 copies) of plasmid. The following primers used for quantitative PCR were 1ab-F: 5'-AGAAGATTGGTTAGATGATGATAGT-3'; 1ab-R: 5'-TTCCATCTCTAATTGAGGTTGAACC-3'; and probe 5'-FAM-TCCTCACTGCCGTCTTGTTG ACCA-BHQ1-3'.

All experiments were conducted in triplicates. Relative expression was estimated using the $2^{-\Delta\Delta Ct}$ method.

Infection of Hamster Rat

Hamster rat used as COVID-19 model as previously reported (*5*), 12 rats were divided into 4 groups with three rat each, then rats were infected intranasally with SARS-CoV-2 (1×10^5 PFU) in a total volume of 50 μL. 1 h post infection, rat received NK007(*S*, *R*) or Remdesivir via intranasal dropping in a volume of 50 μL, an equivalent volume of NS was administered as a control. Rats received NK007(*S*, *R*) or Remdesivir or NS treatment for 3 days. All mice were weighted at every day and euthanized at 4dpi. The lung homogenates were weighed and prepared in differential volume of NS (0.1 g tissue with 0.5 mL NS) and trituration for 10 min and then centrifuged at 3000 rpm for 10 min at 4 ℃. The 100 μL supernatant of lung homogenates were collected to extract viral RNA and qRT-PCR were used to assess the SARS-CoV-2 RNA copies.

Histopathological Examination of Rats

Animals were anesthetized and the lungs were fixed in 4% (v/v) paraformaldehyde solution for 48 hours, and the paraffin sections (3-4 μm) were prepared routinely. The paraffin sections were

stained with Hematoxylin and Eosin (H&E) to identify histopathological changes in the lungs. The histopathology of the lung tissue was observed by light microscopy.

All work with SARS-CoV-2 was conducted in the Biosafety Level 3 (BSL3) Laboratories of National Institute for Viral Disease Control & Prevention, Chinese Center for Disease Control and Prevention.

Tables and Figures

Table S1.
Determination of the EC_{50} value of NK007(*S*, *R*).

Concn.μM	5	0.5	0.05	0.005	0.0005	0.00005	virus
Ct Value	30.41	30.63	22.96	15.08	15.21	15.06	15.06
	30.26	30.24	22.63	15.12	15.09	15.02	15.38
	30.72	30.35	22.62	15.26	15.87	15.1	14.56

Table S2.
Determination of the EC_{50} value of remdesivir.

Concn.μM	100	20	4	0.8	0.16	0.032	virus
Ct Value	32.45	31.34	29.35	15.89	15.21	14.5	15.06
	32.25	31.67	29.74	15.99	15.18	15.46	15.38
	32.79	31.48	29.67	16.25	15.42	14.99	14.56

Table S3.
Determination of the CC_{50} value of NK007(*S*, *R*).

Concn.μM	mock	1000	200	40	8	1.6	0.32	0.064	0.0128	0.00256
Value of OD490	2.0571	0.4746	1.0158	1.2791	1.3669	1.5232	1.7838	2.0714	2.0516	2.0489
	2.062	0.6044	0.9834	1.2413	1.5081	1.6269	1.8645	1.9628	2.0438	2.0751
	2.0571	0.6759	0.9315	1.3092	1.4573	1.6698	1.7395	1.9218	2.0378	2.0494

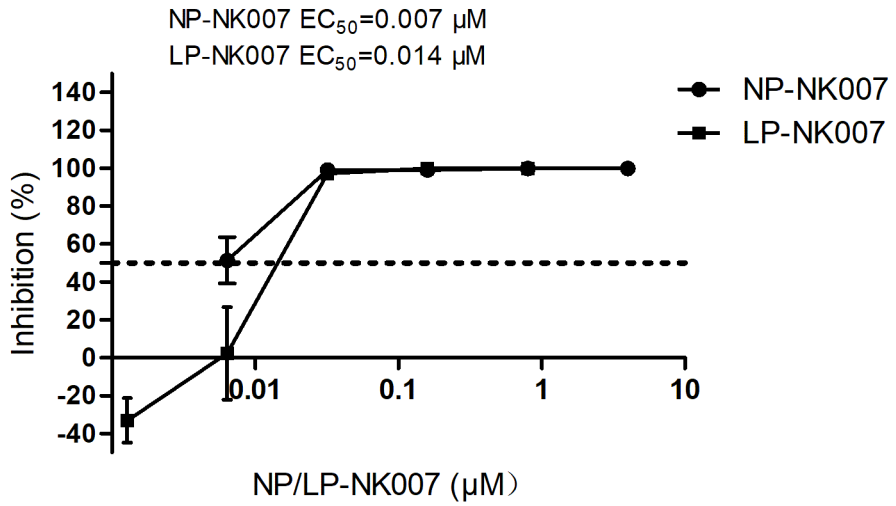

Figure S1. EC_{50} values of NP-NK007 and LP-NK007. NP-NK007 EC_{50}=0.007 μM, LP-NK007 EC_{50}=0.014 μM.

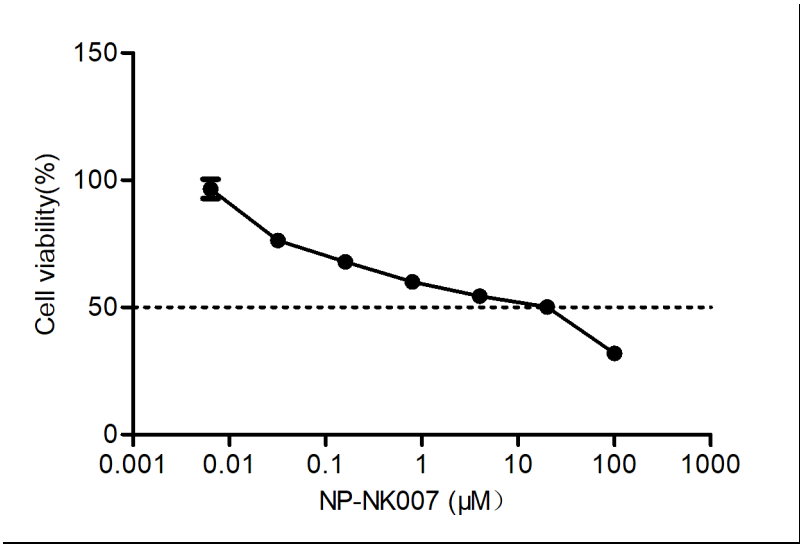

Figure S2. CC_{50} value of NP-NK007. NP-NK007 CC_{50}≈20 μM.

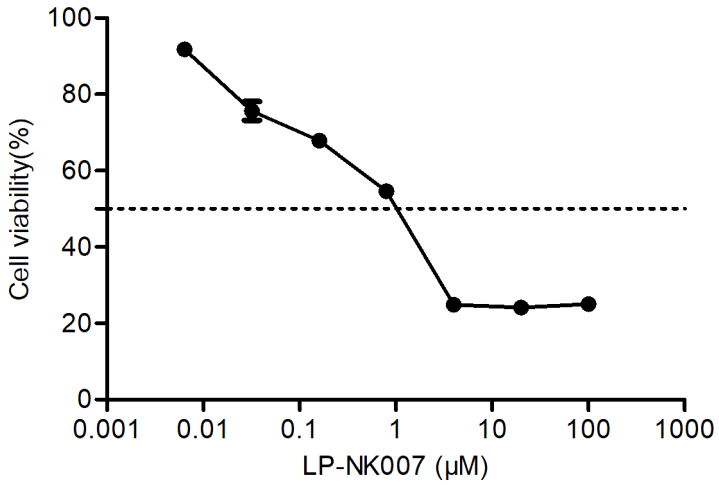

Figure S3. CC_{50} value of LP-NK007. LP-NK007 CC_{50}≈1 μM.

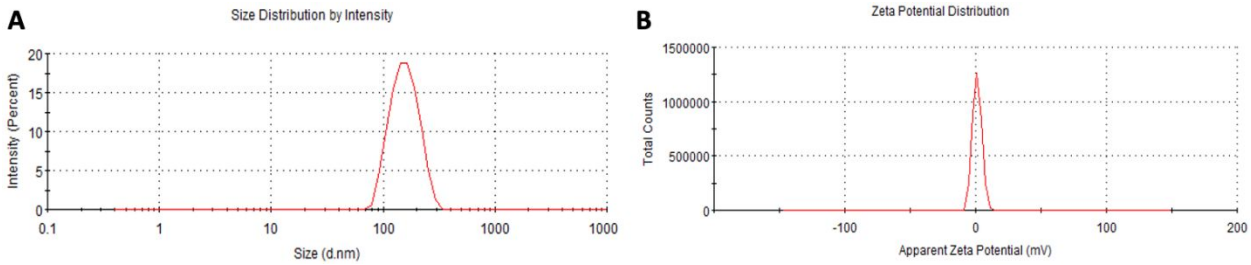

Figure S4. The representative size distribution (A) and zeta potential (B) of NP-NK007.

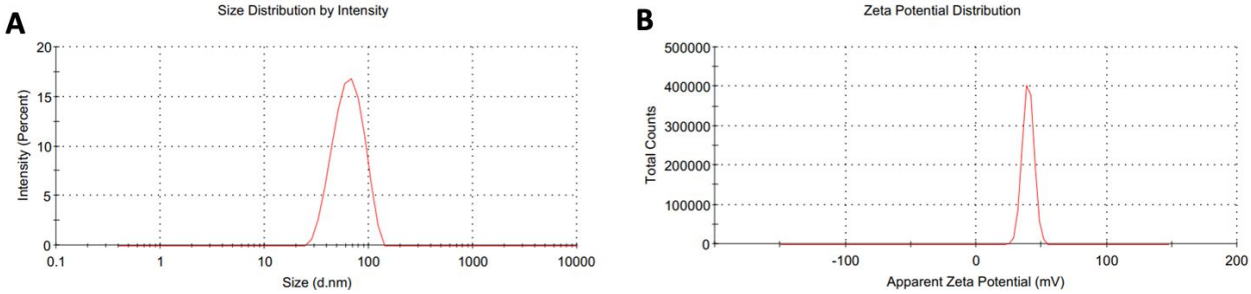

Figure S5. The representative size distribution (A) and zeta potential (B) of LP-NK007.

References

1. Wang, K.; Su, B.; Wang, Z.; Wu, M.; Li, Z.; Hu, Y.; Fan, Z.; Mi, N.; Wang, Q. Synthesis and antiviral activities of phenanthroindolizidine alkaloids and their derivatives. *J. Agric. Food. Chem.* **2010**, *58*, 2703–2709.

2. Zhao, S.; Li, J.; Zhou, Y.; Huang, L.; Li, Y.; Xu, J.; Fu, C.; Guo, X.; Yang, J. Lipid nanoparticles-encapsulated YF4: A potential therapeutic oral peptide delivery system for hypertension treatment. *Front Pharmacol* **2019**, *10*, 102.

3. Shabnam, K.; Mehrab, P.; Fatemeh, Y.; Ghadami, A. The synthesis and characterization of targeted delivery curcumin using chitosan-magnetite-reduced graphene oxide as nano-carrier. *Int. J. Biol. Macromol. 2021*, *186*, 554−562.

4. Yao, X.; Ye, F.; Zhang, M.; Cui, C.; Huang, B.; Niu, P.; Liu, X.; Zhao, L.; Dong, E.; Song, C.; Zhan, S.; Lu, R.; Li, H.; Tan, W.; Liu, D. In vitro antiviral activity and projection of optimized dosing design of hydroxychloroquine for the treatment of severe acute respiratory syndrome coronavirus 2 (SARS-CoV-2). *Clin. Infect. Dis.* **2020**, *71*, 732−739.

5. Sia, S.; Yan, L.; Chin, A.; Fung, K.; Choy, K.; Wong, A.; Kaewpreedee, P.; Perera, R.; Poon, L.; Nicholls, J.; Peiris, M.; Yen, H. Pathogenesis and transmission of SARS-CoV-2 in golden hamsters. *Nature* **2020**, *583*, 834–838.